

# Corrosion behaviour of $R_2O$ – $CaO$ – $SiO_2$ glasses submitted to accelerated weathering

N. Carmona<sup>a,\*</sup>, M. A. Villegas<sup>b</sup>, J. M. Fernández Navarro<sup>c</sup>

<sup>a</sup> *Fundación Centro Nacional del Vidrio, Real Fábrica de Cristales de San Ildefonso, Po Pocillo, 1, 40100 La Granja, Segovia, Spain*

<sup>b</sup> *CENIM, Spanish Council for Scientific Research, CSIC, Avda. Gregorio del Amo, 8, 28040 Madrid, Spain*

<sup>c</sup> *Institute of Optics, Spanish Council for Scientific Research, CSIC, C. Serrano, 121, 28006 Madrid, Spain*

Received 18 January 2004; received in revised form 19 April 2004; accepted 1 May 2004

Available online 28 July 2004

## Abstract

Four glasses in the  $R_2O$ – $CaO$ – $SiO_2$  ( $R = Na, K$ ) system, following similar compositions to historical glasses used for production of stained glass windows, were prepared with different  $CaO/R_2O$  ratio. The samples were submitted to accelerated weathering test under different temperature and relative humidity conditions, as well as under controlled  $SO_2$ -polluted atmosphere. The experimental set up was selected to simulate the main conditions responsible for the deep deterioration submitted by the historical stained glass windows. Such damage has been very important during the last century, as a consequence of highly polluted industrial environments.

As far as the results concern, it has been shown that 400 cycles of variable temperature and humidity are capable to develop pits on the glass surface, its shape and intensity depending on the glass composition. When weathering cycles were carried out with 10 ppm  $SO_2$  under high humidity conditions, calcium carbonate crystals appeared upon the glass surface, whereas calcium sulphate crystallisation occurred for higher  $SO_2$  concentration. The mechanism of chemical damage has been proposed and discussed in terms of the reaction between the  $Ca^{2+}$ -ions leached from the glass sample and the environmental  $SO_2$ . The former whole reaction occurred through an intermediate stage: the calcium carbonate crystallisation. That salt was displaced by sulphate only when the  $SO_2$  concentration was high enough.

© 2004 Elsevier Ltd. All rights reserved.

**Keywords:** Electron microscopy; Corrosion; Glass;  $SiO_2$ ; Historical glass windows; Weathering

## 1. Introduction

During the last decades many studies about the characterisation of historical glasses corrosion have been carried out.<sup>1–5</sup> A special interest is paid to glasses from stained glass windows, since they have been submitted to a long damaging time during the last centuries. Different corrosion behaviour has been recorded in that glasses depending on their chemical composition and weathering conditions. The atmospheric pollutants nature and concentration have determined the deterioration pattern of glasses from stained glass windows. Nowadays atmospheric  $SO_2$  concentration has been reduced and tends to decrease even more, but stained glass windows were deeply damaged for many decades when the pollutants level was not especially controlled. As a consequence, stained glasses have developed thick crusts of salt

deposits, pits and other decay signs that dealt with the loss of their artistic and historical value.

To the best of the authors knowledge, up to now only calcium sulphate was reported as the main salt component in corrosion crusts upon historical stained glasses.<sup>6–12</sup> In some others studies about glass behaviour in natural groundwater,  $HCO_3^-$  anions were found in the initial corrosion stage.<sup>13,14</sup> This research was motivated by the fact that calcium carbonate instead of calcium sulphate were detected on historical glass samples from the Cathedral of León (13th century, Spain).<sup>14</sup> Those glasses were removed from the stained glass windows in the last whole restoration carried out during the 19th century. Therefore, the glass pieces were kept indoor and preserved from the environmental aggressiveness (gaseous pollutants from industries and roaded traffic, mainly). With the aim to perform a detailed study about the corrosion mechanism submitted by the stained glasses, a set of simulated weathering experiments were planned. Likewise, several glasses with similar compositions to the Medieval and Renaissance ones,<sup>16–18</sup> were prepared at the

\* Corresponding author. Tel.: +49 931 4100 705;

fax: +49 931 4100 799.

E-mail address: [carmona@isc.fhg.de](mailto:carmona@isc.fhg.de) (N. Carmona).

laboratory in order to be tested following the former weathering experiments. In such glasses, the potash content was varied as well as the CaO/K<sub>2</sub>O molar ratio, which has been discussed to be the most important parameter in determining chemical stability of historical glasses.<sup>16–22</sup> Summarising, the objective of the present work was to monitor the mechanism of chemical degradation of old glass compositions similar to that of the stained glass windows of the Cathedral of León. With the aim to attain valuable results in a reasonable period of time, accelerated corrosion tests were carried out. Variable parameters, such as temperature, relative humidity and ultraviolet light as well as SO<sub>2</sub> concentration, playing an important role in the glass decay process, were controlled.

## 2. Experimental

### 2.1. Preparation and characterisation of glasses

Since original historical glass samples are limited by obvious conservation reasons, this research was conducted on glasses obtained at the laboratory, following several model compositions of Medieval and Renaissance glasses used in the past to produce stained glass windows.<sup>15–17</sup> Four glasses were prepared with the compositions summarised in Table 1. Both weight and molar percentage are shown: formulation as weight percent is the current way in which the glasses composition is expressed by the industrial sector, while molar percentage is more self-explaining from the chemical point of view, for instance to discuss the ratio between the different glass components.

Glass G1 composition approximately corresponds to a soda lime silicate conventional glass, nowadays used for architectural applications (windows) and also similar to that of the glass windows used in the Renaissance period. This glass composition is characterised by a high silica percentage and an equilibrated ratio between R<sub>2</sub>O (alkaline oxides) and CaO. All the other three glasses (G2, G3 and G4, Table 1) are similar to medieval glasses frequently used for production of stained glass windows. They were formulated following the same base composition and varying the mo-

lar ratio R<sub>2</sub>O/CaO. Moreover, in all the prepared glasses 1.0 wt.% MnO was added, with the aim to verify if, due to the well known solarisation phenomenon<sup>23</sup> in MnO containing glasses, a darkening process takes place. Thus, by introducing this oxide it was possible to monitorise simultaneously chemical degradation and, if any, photooxidation during the ageing cycles.

All the glasses were prepared starting from pure chemical reagents (analytical grade) and from washed quartz sand. The melting was carried out in an electrical furnace up to 1400 °C for 2 h. After that the glasses were cast and hand-pressed to obtain 3–4 thick plates (5 cm). Once the glasses were slowly cooled down (350 °C/h), samples of 1.5 cm × 2.5 cm × 0.4 cm in size were cutted off.

Some physical properties of the glasses were determined: linear expansion coefficient ( $\alpha$ ),<sup>23,24</sup> glass transition temperature ( $T_g$ )<sup>23,25</sup> and wavelength at the absorption maximum ( $\lambda_{max}$ ).<sup>20</sup> Linear expansion coefficient and transition temperature were determined from the corresponding dilatometric curves obtained with a differential dilatometer Netzsch model 402EP. Ultraviolet-visible (UV-vis) spectra were recorded with a Perkin-Elmer Lambda 19 spectrophotometer in the 300–800 nm range.

### 2.2. Accelerated weathering tests

To study the behaviour of the former glasses under different conditions of temperature, relative humidity (RH) and UV radiation as a function of time (weathering-1 test), the samples were submitted to ageing cycles inside a Minitest CCM-25/81 chamber. This chamber is provided with an UV lamp (Philips MLW, 160 W). The ageing cycles (7 h each) simulated a humid (80% RH) and very warm (60 °C) climate, together with UV radiation for the first 3 h. A very dry (30% RH) and cold (–15 °C) simulated climate without UV radiation completed the ageing cycle.

Two more ageing cycles (weathering-2 and weathering-3) were conducted with different SO<sub>2</sub> concentration as the main responsible for the deep chemical damage submitted by the historical stained glasses during the last century.<sup>26,27</sup> In this case a Kesternich chamber mod. VCK-300 was used,

Table 1  
Chemical composition (mol% and wt.%) of the glasses prepared

Oxides	mol%				wt.%			
	Glass 1	Glass 2	Glass 3	Glass 4	Glass 1	Glass 2	Glass 3	Glass 4
P <sub>2</sub> O <sub>5</sub>	–	1.5	1.5	1.5	–	3.4	3.3	3.3
SiO <sub>2</sub>	72.0	50.0	50.0	50.0	71.9	48.4	47.2	46.1
Al <sub>2</sub> O <sub>3</sub>	1.0	1.5	1.5	1.5	1.7	2.5	2.4	2.3
MgO	2.0	5.0	5.0	5.0	1.3	3.2	3.2	3.1
CaO	8.0	33.5	29.5	25.5	7.4	30.3	26.0	21.9
MnO	1.0	1.0	1.0	1.0	1.2	1.1	1.1	1.1
Na <sub>2</sub> O	16.0	0.5	0.5	0.5	16.5	0.5	0.5	0.5
K <sub>2</sub> O	–	7.0	11.0	15.0	–	10.6	16.3	21.7
R <sub>2</sub> O/CaO, R = Na, K	2.0	0.2	0.4	0.6	–	0.4	0.6	1.0

which can control SO<sub>2</sub> concentration in the 10–3000 ppm range. For these experiments, the temperature was 40 °C, the RH 100% and the cycle time was 24 h. The corresponding SO<sub>2</sub> dose (10 ppm for weathering-2 test and 1800 ppm for weathering-3 test) was introduced in the chamber at the beginning of the ageing cycle. Obviously, the two SO<sub>2</sub> concentrations tested were very high in comparison with the present atmospheric SO<sub>2</sub> content in industrial towns. For instance, SO<sub>2</sub> level in both Madrid (Spain, dry environment) and Cracow (Poland, humid environment) is below 0.1 ppm.

Superficial deterioration of samples was directly observed by optical microscopy with a Nikon mod. SMZ-2T and Nikon mod. Optiphot2-POL equipment attached with an accessory to take micrographs. Scanning electron microscopy (SEM) (Philips XL30) was used to undertake a detailed study of the surface morphology. Likewise, microanalyses were performed by energy dispersive X-ray spectrometry (EDX) with a DX4i analyser attached to the former microscope.

The crystalline corrosion products obtained after the accelerated weathering tests were detected by X-ray diffraction (XRD) with a Siemens D5000 diffractometer, provided with a Kristalloflex 710 generator. The copper K $\alpha$ 1 radiation ( $\lambda = 0.15405$  nm) with a nickel filter and a 0.1 mm detector collimator were used at 50 kV and 30 mA.

### 3. Results and discussion

#### 3.1. Properties of glasses

Table 2 summarises the physical properties determined in the glass samples. The linear expansion coefficient ( $\alpha$ ), measured between 20 and 300 °C,<sup>23,24</sup> increases with the K<sub>2</sub>O molar percentage in potash-lime silicate glasses. This fact can be explained by the progressive incorporation of K<sub>2</sub>O that diminishes the structural cohesion and allows the formation of a more open and weaker glass network. In addition, the glass transition temperature ( $T_g$ ) tends to diminish when CaO was substituted by K<sub>2</sub>O, due to the same reasons.

The absorption spectra of the studied glasses in the visible range showed a maximum at about 499 nm. This absorption band corresponds to the characteristic optical feature of Mn<sup>3+</sup>-ions,<sup>23</sup> responsible for the violet colouring of the glasses prepared. By comparing the maximum absorption wavelengths of the spectra of the three potash-lime glasses (G2, G3 and G4), a shift towards longer wavelengths is recorded when the R<sub>2</sub>O/CaO molar ratio increased. The ra-

tio Mn<sup>2+</sup>/Mn<sup>3+</sup> decreases in the same sense that the glass basicity increases, i.e. the molar ratio R<sub>2</sub>O/CaO in the sequence G2 < G3 < G4. This explains the more deeper violet colouring in the glass G4 and its more shifted absorption band.

#### 3.2. Accelerated weathering

##### 3.2.1. Weathering-1: Tests under variable temperature and RH

Visible absorption spectra of glasses recorded both before and after 400 accelerated weathering-1 cycles were invariable. This means that, during the tests, UV exposure has not oxidised Mn<sup>2+</sup>-ions to Mn<sup>3+</sup>-ions, and thus no solarisation effect took place. On the contrary, the temperature and RH changes dealt with a deep attack on the glass G1 (Fig. 1a). Upon the surface of this glass, isolated pits appeared with a dark central nucleus and a clear rounding area. Smaller pits were also observed with different aggregation degree upon the former pits. Microanalyses performed on that surface (W1A1G1, weathering-1, analysis 1, glass 1; Table 3) shows a decreasing in the Na<sub>2</sub>O content, in comparison with the Na<sub>2</sub>O concentration in the original glass, and a consistent relative increase of the other components. In the potash-lime glasses G2, G3 and G4, the deterioration begins later. The higher is the K<sub>2</sub>O content, the higher is the chemical attack observed. Fig. 1b–d show, respectively, the surface morphology of those glasses. The microanalyses carried out on that surfaces showed a small decreasing of the silica content, a light relative increasing of CaO and almost the same amount of K<sub>2</sub>O (analysis W1A1G2 for glass 2, W1A1G3 for glass 3 and W1A1G4 for glass 4; Table 3).

In all the glasses tested hydrolytic attack took place. It begins by the ion-exchange of H<sup>+</sup>-ions from the atmospheric water with the alkaline-ions ( $R^+ = Na^+, K^+$ ) from the glass surface (Fig. 2, step 1). Although a priori it would be expected that glass G1 will show a good hydrolytic resistance (due to the lower leaching tendency of Na<sup>+</sup>-ions in comparison with K<sup>+</sup>-ions from the potash-lime glasses G2, G3 and G4), this soda-lime silicate glass G1 is the most damaged one. The higher deterioration observed in glass G1

Table 2  
Some physical properties of the glasses prepared

Glass	$\alpha$ ( $\times 10^{-7}$ K <sup>-1</sup> ) (20–300 °C)	$T_g$ (°C)	$\lambda_{max}$ (nm)
G1	98.3	530	484
G2	98.4	716	478
G3	104.7	621	481
G4	111.8	632	498

Table 3  
EDX microanalyses performed on the glasses submitted to the weathering-1 tests (400 cycles with variable temperature and RH) (wt.%)

Oxides	W1A1G1 <sup>a</sup>	W1A1G2	W1A1G3	W1A1G4
P <sub>2</sub> O <sub>5</sub>	–	2.6	3.1	2.8
SiO <sub>2</sub>	79.4	38.9	39.0	41.6
Al <sub>2</sub> O <sub>3</sub>	2.6	7.4	5.3	3.2
MgO	1.7	2.0	2.5	0.2
CaO	9.3	35.5	30.6	26.6
MnO	2.4	1.9	2.0	1.4
Na <sub>2</sub> O	4.2	1.0	1.0	0.0
K <sub>2</sub> O	–	10.2	16.1	24.0
Cl <sup>-</sup>	0.4	0.4	0.4	0.2

<sup>a</sup> W: weathering; A: analysis; G: glass.

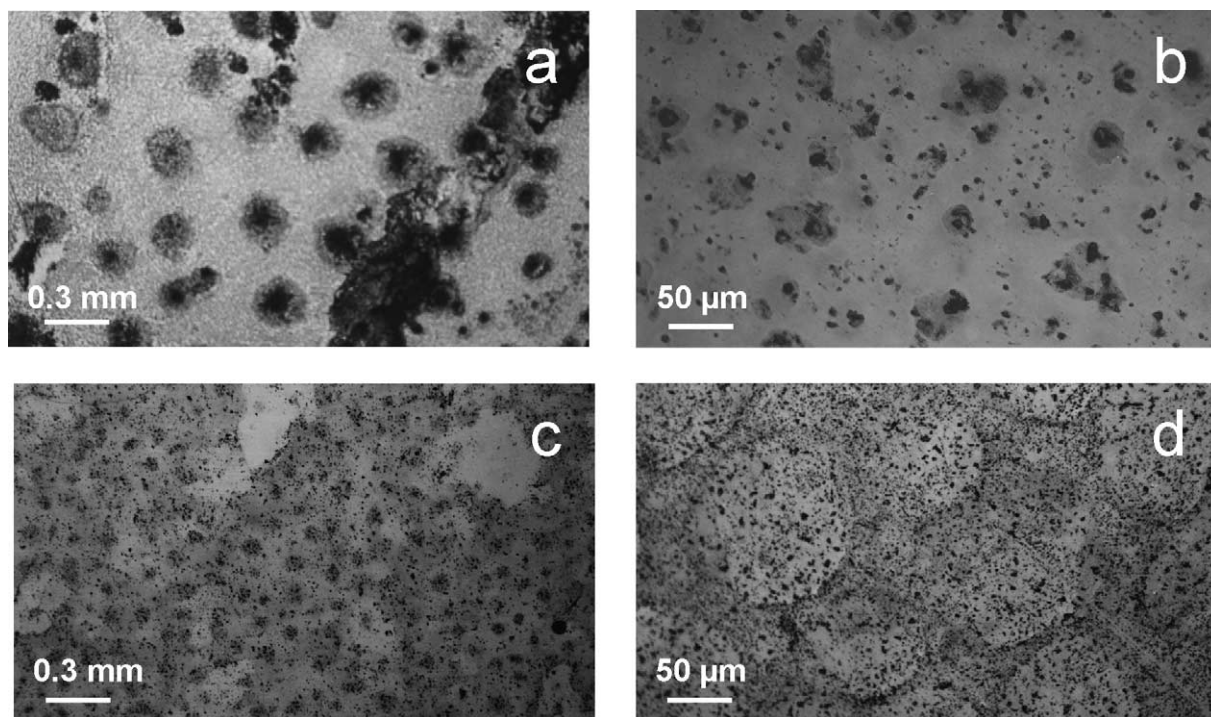


Fig. 1. Optical microscopy images of the glasses surface: (a) G1, (b) G2, (c) G3 and (d) G4, after 400 weathering cycles performed under variable temperature and relative humidity (weathering-1).

can be explained on the basis of its alkaline oxide content (16.0 mol%, Table 1) which is higher than the  $K_2O$  content in glass G2 (7.0 mol%), G3 (11.0 mol%) and G4 (15.0 mol%). Moreover, in the three potash-lime glasses the  $CaO$  amount (which behaves as a network stabilising oxide) varies between 33.5 and 25.5 mol%, while in the soda-lime glass G1 the calcium oxide content is much lower (about 8.0 mol%). The two reasons stated above explain why glass G1 showed more damage signs than glasses G2, G3 and G4. Such a damage is exclusively attributed to a dealkalinisation process as a consequence of the ion-exchange enhanced by the environmental hydrolytic attack. In fact, it has been

confirmed that common soda-lime silicate glass submits a strong interaction with water,<sup>28,29</sup> and, on the other hand, they are classified as a *hydrolytic class 3* glass, according to the ISO standard for hydrolytic resistance.<sup>30</sup> EDX microanalyses performed on the surface of the glass G1, once submitted to the weathering-1 test, confirmed a noticeable decreasing in the  $Na_2O$  content and a relative increasing of the silica content. This agrees with the superficial dealkalinisation process explained above.

### 3.2.2. Weathering-2: Tests under 10 ppm $SO_2$

After 95 cycles under 10 ppm  $SO_2$  atmosphere, the surface of glass G1 does not show important deterioration (Fig. 3a). The corresponding EDX microanalysis (W2A1G1, Table 4) indicated that the glass composition at the surface is almost the same than those of the inner part of the glass (a light  $Na_2O$  decrease was recorded). In the glasses G2, G3 and G4, the higher is their  $K_2O$  content, the higher is the damage produced after this weathering test (Fig. 3b–d). The EDX microanalyses carried out on different areas of the glasses surface, showed white needle shaped crystals in which the calcium content is high (W2A2G2, W2A2G3 and W2A2G4; Table 4). Further qualitative chemical analyses performed on the white crystals, demonstrated their nature to be calcium carbonate.

The EDX microanalyses corresponding to the superficial areas without crystals (W2A1G2, W2A1G3 and W2A1G4; Table 4), indicated that the  $MgO$  and  $CaO$  contents were reduced due to their leaching and precipitation as, for in-

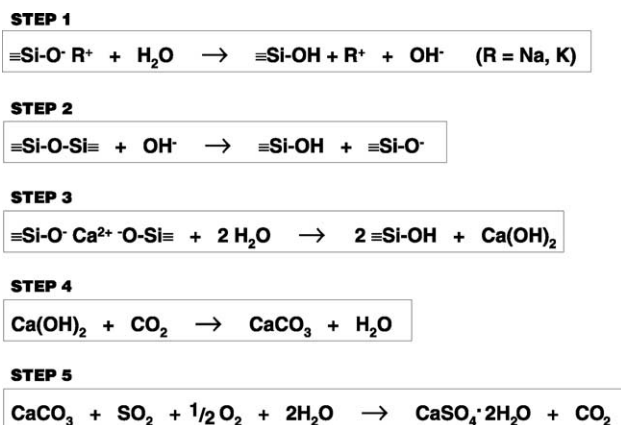


Fig. 2. Steps of the chemical deterioration mechanism for the glasses studied.

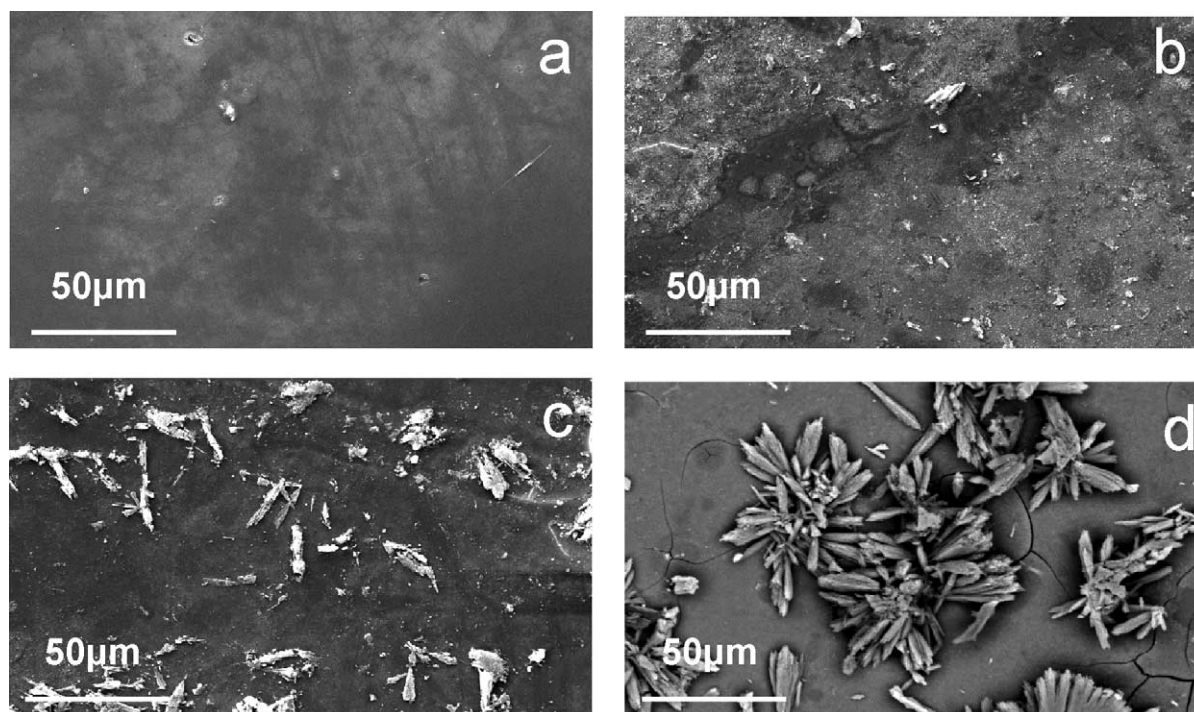


Fig. 3. SEM images of the glasses surface: (a) G1, (b) G2, (c) G3 and (d) G4, after 95 weathering cycles under 10 ppm SO<sub>2</sub> each (weathering-2).

stance, calcium carbonate. Consequently, the silica and the alumina contents show a relative increase. In addition, the MnO amount was maintained. The K<sub>2</sub>O amount was found to be strongly reduced, due to the ion-exchange between K<sup>+</sup>-ions and H<sup>+</sup>-ions from the water. After reaction with SO<sub>2</sub>, potassium sulphate was formed, washed off because of its high solubility in aqueous medium and detected after each cycle on the tray at the bottom of the tests chamber.

It is important to note that after the aggressive conditions of the weathering-2 test, corrosion crusts are formed upon potash-lime glasses G2, G3 and G4; and that such a crusts were composed by calcium carbonate, instead of calcium sulphate, as it would be expected following former literature reports on crusts found on medieval stained glasses weathered under humid and polluted environments.<sup>11–13</sup> Moreover, Ojovan et al.,<sup>14</sup> found HCO<sub>3</sub><sup>−</sup> ions as a leaching intermediate product of glasses used for nuclear waste immobilisation, which indirectly support our results.

### 3.2.3. Weathering-3: Tests under 1800 ppm SO<sub>2</sub>

With the aim to intensify the weathering conditions under which calcium sulphate may appear in the corrosion crusts, tests under 1800 ppm SO<sub>2</sub> were conducted. After such weathering test, glass G1 did not show relevant deterioration, while potash-lime glasses G2, G3 and G4 were seriously damaged (Fig. 4). These glasses appeared completely covered by a thick white corrosion crust (~2 mm thickness). The crust was spongy in glass G2 and more compact and adhered to the glass surface in samples G3 and G4.

SEM micrographs (Fig. 4a–c) show longed crystals of calcium sulphate, as indicated the EDX microanalyses performed on the corresponding glass surfaces (W3A1G2, W3A1G3 and W3A1G4; Table 5). The corrosion crusts formed were carefully removed with a scalpel and analysed by XRD. The results obtained showed that gypsum with a low crystallinity degree is present in the glass G2 crust; with medium crystallinity degree in the glass G3 crust; and

Table 4

EDX microanalyses performed on the glasses submitted to the weathering-2 tests (95 cycles under 10 ppm SO<sub>2</sub> each) (wt.%)

Oxides	W2A1G1	W2A1G2	W2A2G2	W2A1G3	W2A2G3	W2A1G4	W2A2G4
P <sub>2</sub> O <sub>5</sub>	–	3.9	6.8	3.4	5.9	5.2	5.3
SiO <sub>2</sub>	74.0	52.4	44.4	62.3	31.8	58.3	2.6
Al <sub>2</sub> O <sub>3</sub>	3.0	10.0	10.0	7.1	4.3	4.7	0.6
MgO	2.2	2.4	3.7	2.4	2.1	2.3	2.7
CaO	6.8	22.3	29.0	14.6	47.8	16.1	84.3
MnO	1.2	1.1	1.6	1.6	1.8	1.6	2.5
Na <sub>2</sub> O	12.8	–	–	–	–	–	–
K <sub>2</sub> O	–	7.5	4.5	8.0	2.9	11.6	1.2
SO <sub>3</sub>	–	0.4	–	0.6	3.4	0.2	0.8

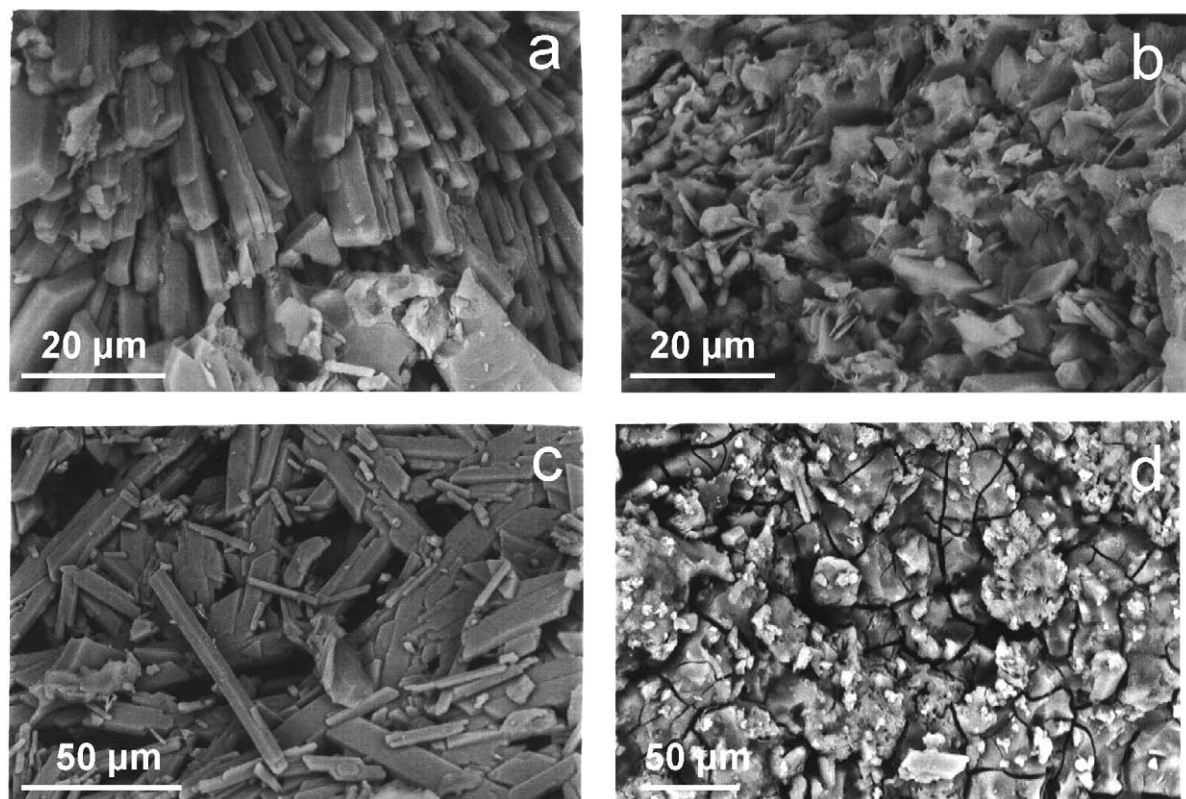


Fig. 4. SEM images of corrosion crusts of glasses: (a) G2, (b) G3 and (c) G4, after 15 weathering cycles under 1800 ppm  $\text{SO}_2$  each; (d) image of glass G2 surface once the corrosion crust was removed.

well crystallised in the glass G4 crust. Some amorphous silica grains were detected as well. Once the crusts were removed, a very cracked surface was observed in the three potassic glasses (Fig. 4d). EDX microanalyses of such surfaces showed that both  $\text{CaO}$  and  $\text{K}_2\text{O}$  have been almost released and the silica content appeared proportionally increased (W3A2G3 on the glass G3 surface and W3A2G4 on the glass G4 surface; Table 5). The weathering-3 test, with a so very high  $\text{SO}_2$  concentration, demonstrated that only when the  $\text{SO}_2$  content is high enough, the calcium sulphate corrosion crusts appear on the glass surface.

The different weathering tests performed on the four glasses prepared and studied, have pointed out the chem-

ical deterioration mechanism and the steps with which it proceeds. As is said above, the first step is a hydrolytic attack that takes place by ion-exchange between the  $\text{H}^+$ -ions from the water and  $\text{R}^+$ -ions from the glass surface (Fig. 2, step 1). When  $\text{SO}_2$  is present ( $\sim 10$  ppm) as an atmospheric pollutant, the higher is the  $\text{CaO}$  content, the higher are the corrosion crusts formed. In the glasses studied, the alkaline hydroxide ( $\text{KOH}$  or  $\text{NaOH}$ ) formed, as a consequence of the ion-exchange, interacts with the siloxane bonds ( $\equiv\text{Si}-\text{O}-\text{Si}\equiv$ ) of the glass and destroys the network. This deals with the glass depolymerisation, especially in the case of  $\text{KOH}$  formation which is a stronger basic hydroxide than  $\text{NaOH}$  (Fig. 2, step 2). Once the glass network is broken down,  $\text{Ca}^{2+}$ -ions leaching as  $\text{Ca}(\text{OH})_2$  is enhanced (Fig. 2, step 3). The next step is the carbonation of calcium hydroxide under low and medium ( $\sim 10$  ppm)  $\text{SO}_2$  concentration (Fig. 2, step 4). Finally, only under highly  $\text{SO}_2$  concentrated environments or after a long exposure under  $\text{SO}_2$  polluted atmosphere, carbonate ions can be displaced by sulphate ions that will form anhydrous or hydrated calcium sulphate (Fig. 2, step 5).

#### 4. Conclusions

When temperature and humidity are the only weathering test variables, glass G1 (soda lime silicate) was the most

Table 5

EDX microanalyses performed on the glasses submitted to the weathering-3 test (15 cycles under 1800 ppm  $\text{SO}_2$  each) (wt.%)

Oxides	W3A1G2	W3A1G3	W3A2G3	W3A1G4	W3A2G4
$\text{P}_2\text{O}_5$	–	3.6	1.4	2.1	2.5
$\text{SiO}_2$	–	21.7	77.0	33.0	84.4
$\text{Al}_2\text{O}_3$	–	1.7	3.6	1.7	1.6
$\text{MgO}$	–	0.8	0.4	0.5	0.3
$\text{CaO}$	38.8	24.8	3.6	24.2	0.6
$\text{MnO}$	–	1.1	0.5	–	0.6
$\text{Na}_2\text{O}$	–	1.3	0.5	–	0.4
$\text{K}_2\text{O}$	–	2.4	3.7	1.7	2.5
$\text{SO}_3$	61.2	42.6	9.3	36.8	7.1

damaged. In potash-lime silicate glasses, the higher is the  $K_2O$  content, the higher is the hydrolytic attack produced. These facts can be explained taking into account both the alkaline and alkaline-earth oxides content in the glasses, i.e. the molar ratio  $R_2O/CaO$ . The network stabilising role of the alkaline-earth oxides have to be considered to explain the hydrolytic resistance of glasses, especially in potash-lime glasses.

The ultraviolet irradiation during the weathering tests did not produce an increase of the visible absorbance attributable to the  $Mn^{2+}$ -ions photooxidation. Therefore, under the experimental conditions tested, no solarisation phenomenon occurs.

$SO_2$  presence during weathering tests is a very important factor for the glass chemical deterioration. Weathering tests with 10 ppm  $SO_2$  affected in low extent to soda lime glass, in which only the ion-exchange of  $Na^+$ -ions with  $H^+$ -ions from the moisture water was observed. However, potash-lime glasses were easily damaged under a 10 ppm  $SO_2$  environment. Firstly thick  $CaCO_3$  corrosion crusts are formed. In this case a double chemical mechanism takes place: (i) ion-exchange of  $K^+$ -ions from the glass with  $H^+$ -ions from the moisture water; and (ii) glass network depolymerisation performed by the alkaline attack of the in situ KOH formed. When the glass depolymerisation occurs,  $Ca^{2+}$ -ions leaching as  $Ca(OH)_2$  also takes place, which forms  $CaCO_3$  when in contact with the atmospheric  $CO_2$ . Calcium sulphate precipitation was observed when the  $SO_2$  concentration during the weathering test was high enough. In such a case carbonate ions are displaced by sulphate ions.

To the best of the authors knowledge, up to now the formation of  $CaCO_3$  as an intermediate step in the precipitation of  $CaSO_4$  on the corrosion crusts, has not been reported. Calcium carbonate does not appear in the literature related to neither historical glasses analyses nor simulated accelerated weathering tests with model glasses from the laboratory. Thus,  $CaCO_3$  is firstly formed and thereafter displacement of carbonate-ions by sulphate-ions takes place. The present work demonstrates that under moderate to medium polluted environments, the corrosion crusts upon potash-lime glasses are formed by  $CaCO_3$ . Nevertheless, more experimental work, nowadays in progress, must be done to clarify the critical  $SO_2$  threshold under which the glass corrosion proceeds.

## Acknowledgements

The authors wish to thank EC-FEDER-CICYT for financing the project 2FD97-0418.

## References

1. Fernández Navarro, J. M., Procesos de alteración de vidrieras medievales. Estudios y tratamientos de protección. *Mater. Construcc.*, 1996, **46**, 5–25, 242–243.
2. Fernández Navarro, J. M., Causas del deterioro físico y químico de los vidrios históricos. *Jornadas Naciones sobre Restauración y Conservación de Vidrios*, San Ildefonso, 2000, 17–37.
3. Sterpenich, J. and Libourel, G., Les vitraux médiévaux: caractérisation physico-chimie de l'alteration. *Technique* 1997, **6**, 70–78.
4. García-Heras, M., Gil, C., Carmona, N. and Villegas, M. A., Weathering effects on materials from historical stained glass windows. *Mater. Construcc.* 2003, **53**, 21–34.
5. Guillies, K. J. S. and Cox, A., Decay of medieval stained glass at York, Canterbury and Carlisle. Part 1. Composition of the glass and its weathering products. *Glastech. Ber.* 1988, **61**, 75–84.
6. Ferrazzini, J. C., L'influence de la corrosion sur la vitesse de décomposition des verres du Moyen Age. *Verres Réfract.* 1976, **30**, 26–29.
7. Perez y Jorba, M., Dallas, J. P., Bauer, C., Baherze, C. and Martin, J. C., Deterioration of stained glass by atmospheric corrosion and micro-organisms. *J. Mater. Sci.* 1980, **15**, 1640–1647.
8. Douglas, R. W. and Isard, M. A., The action of water and the sulphur dioxide on glass surfaces. *J. Soc. Glass Technol.* 1949, **33**, 289–335.
9. Lefebvre, R.A., Grégoire, M., Derbez, M. and Ausset, P., Origin of sulphated grey crusts on glass in polluted urban atmosphere: stained glass windows of Tous Cathedral (France). *Glastech. Ber. Glass Sci. Technol.* 1998, **71**(3), 75–80.
10. Schreiner, M. and Schmitz, I., Surface analytical investigations on naturally weathered medieval stained glass. *Riv. Staz. Sper. Vetro.* 2000, **6**, 15–22.
11. Shreiner, M., Deterioration of stained medieval glass by atmospheric attack. Pt. 1. Scanning electron microscopic investigations of the weathering phenomena. *Glastech. Ber.* 1988, **61**, 197–204.
12. Fuchs, D. R., The effects of air pollutants on glass. In *The Effects of Air Pollutants on Materials*, ed. D. S. Lee and T. A. McMullen. AEA Workshop, London, 1994, pp. 29–32.
13. Lifanov, F. A., Ojovan, M. I., Stefanovsky, S. V. and Burcl, R., Cold crucible vitrification of NPP operational waste. *Mater. Res. Soc. Symp. Proc.*, 2003, **757**(II.5.13), 1–6.
14. Ojovan, M. I., Ojovan, N. V., Startceva, I. V., Chuiikova, G. N., Golubeva, Z. I. and Barinov, A. S., Waste glass behaviour in a loamy soil of a wet repository site. *J. Nucl. Mater.* 2001, **298**, 174–179.
15. Carmona, N., *Study of Alteration Processes in Stained Glass Windows and Restoration and Protection Treatments*. Ph.D. dissertation, Universidad de Valladolid, July 2002.
16. Bettembourg, J. M., Composition et altération des verres de vitraux anciens. *Verres Réfract.* 1976, **30**, 36–42.
17. Valle, F. J., Ortega, P., Pascual, L., Carmona, N. and Fernández Navarro, J.M., Chemical composition of medieval stained glasses from the cathedral of León (Spain). *Glass Sci. Technol.* 2002, **75**, 152–157.
18. Müller, W., Torge, M. and Adam, K., Ratio of  $CaO/K_2O > 2$  as evidence of a special Rhenish type of medieval stained glass. *Glastech. Ber. Glass Sci. Technol.* 1994, **67**(2), 45–48.
19. Brill, H., The morphology of weathering on historical glasses. *Riv. Staz. Sper. Vetro* 2000, **6**, 7–8.
20. Illife, C. J. and Newton, R. G., Using triangular diagrams to understand the behaviour of medieval glasses. *Verr. Refract.* 1976, **30**(1), 30–34.
21. Newton, R. G. and Paul, A., A new approach to predicting the durability of medieval window glass. *Rev. Archeom.* 1981, **5**, 119–128.
22. Cox, G. A., Heavens, O. S., Newton, R. G. and Pollard, A. M., A study of the weathering behaviour of medieval glass from York Minster. *J. Glass Stud.* 1979, **21**, 54–75.
23. Fernández Navarro, J. M., *El vidrio*, ed. Spanish Council for Scientific Research, CSIC, Madrid, 1985.
24. Spanish Standard UNE 43-702-74, *Ensayos de vidrios. Determinación del coeficiente de dilatación lineal*.
25. Spanish Standard UNE 43-703-78, *Ensayos de vidrio. Determinación dilatométrica de la temperatura de transformación*.
26. Standard DIN 50017, *Methods of Testing in Damp Heat Atmospheres*. DIN, Berlin, 1967.

27. Standard DIN 50018, *Testing in a Saturated Atmosphere in the Presence of Sulphur Dioxide*. DIN, Berlin, 1982.
28. Carmona, N., García-Heras, M., Gil, C. and Villegas, M. A., Deterioro de vidrios en medio submarino.ed. Ayuntamiento de Santoña. Monte Buciero, La conservación del material arqueológico Subacuático vol. 9, Santander, 2003, 327–349.
29. Barbieri, L., Corradi, A. and Lancellotti, I., Thermal and chemical behaviour of different glasses containing steel fly ash and their transformation into glass-ceramics. *J. Eur. Ceram. Soc.* 2002, **22**, 1759–1765.
30. ISO 719, *Glass. Hydrolytic Resistance of Glass Grains at 98°C. Method of Test and Classification*. 1985.